Colloids and Surfaces B: Biointerfaces 205 (2021) 111881

Contents lists available at ScienceDirect

Colloids and Surfaces B: Biointerfaces

journal homepage: www.elsevier.com/locate/colsurfb

Probing the role of nuclear-envelope invaginations in the nuclear-entry route of lipofected DNA by multi-channel 3D confocal microscopy

Gianmarco Ferri [a,1], Giuseppe Fiume [a,d,1], Daniela Pozzi [b], Giulio Caracciolo [b], Francesco Cardarelli [a,c,*]

[a] NEST, Scuola Normale Superiore, Pisa, Italy
[b] Department of Molecular Medicine, Sapienza University of Rome, Rome, Italy
[c] NEST, Istituto Nanoscienze-CNR, Piazza S. Silvestro, 12, I-56127, Pisa, Italy
[d] Ares Genetics GmbH, Vienna, Austria

ARTICLE INFO

Keywords:
Lipofection
Gene delivery
Nuclear architecture
Fluorescent probe
3D confocal reconstruction
FM4-64

ABSTRACT

Nuclear breakdown was found to be the dominant route for DNA entry into the nucleus in actively dividing cells. The possibility that alternative routes contribute to DNA entry into the nucleus, however, cannot be ruled out. Here we address the process of lipofection by monitoring the localization of fluorescently-labelled DNA plasmids at the single-cell level by confocal imaging in living interphase cells. As test formulation we choose the cationic 3β-[N-(N,N-dimethylaminoethane)-carbamoyl] cholesterol (DC-Chol) and the zwitterionic helper lipid dioleoylphosphatidylethanolamine (DOPE) with plasmidic DNA pre-condensed by means of protamine. By exploiting the spectral shift of the fluorescent dye FM4-64 (N-(3-triethylammoniumpropyl)-4-(p-diethylaminophenylhexatrienyl)-pyridinium 2Br) we monitor the position of the nuclear envelope (NE), while concomitantly imaging the whole nucleus (by Hoechst) and the DNA (by Cy3 fluorophore) in a multi-channel 3D confocal imaging experiment. Reported results show that DNA clusters are typically associated with the NE membrane in the form of tubular invaginations spanning the nuclear environment, but not completely trapped within the NE invaginations, i.e. the DNA may use these NE regions as entry-points towards the nucleus. These observations pave the way to investigating the molecular details of the postulated processes for a better exploitation of gene-delivery vectors, particularly for applications in non-dividing cells.

1. Introduction

Effective transfection and gene transfer require not simply the entry of DNA into cells and subsequent transcription from an appropriate promoter, but also a number of intracellular events that allow the DNA to move from the extracellular surface of the cell into and through the cytoplasm, and ultimately across the nuclear envelope (NE) and into the nucleus before any transcription can initiate [1]. This latter step is commonly considered the most substantial barrier to effective transfection. In this regard, Capecchi carried out an elegant set of experiments in 1980 in which he microinjected plasmids into either the nuclear or cytoplasmic compartment of non-dividing cells and assayed their ability to express their gene product [2]. When plasmids were injected into the cytoplasm, 100 % of the injected cells showed no gene expression, but when the plasmids were injected into the nucleus, 50–100 % of cells showed gene expression [2]. Several other groups reported similar findings in multiple cell types in the absence of cell division [3–6]. Worthy of note, however, even in actively-dividing cells microinjection into the cytoplasm takes between 30- and 100-times more plasmid compared with injection into the nucleus to give equivalent levels of gene expression [7,8], confirming that the NE is a major impediment to effective gene transfer. In keeping with this general picture, we recently reported that the nuclear breakdown is a dominant route for DNA entry into the nucleus in actively-dividing CHO-K1 cells [9], an outcome supported by similar evidences obtained by others on additional cell lines including (but not limited to) COS-7, HTC-116, K562, and HeLa [10–14]. We monitored the expression of a genetically-encoded green fluorescent protein (GFP) at the single-cell level, and in real-time, by live-cell confocal imaging. As test formulation we choose the cationic 3β-[N-(*N*,

* Corresponding author at: NEST, Scuola Normale Superiore, Pisa, Italy.
E-mail address: francesco.cardarelli@sns.it (F. Cardarelli).
[1] The authors contributed equally to this work.

https://doi.org/10.1016/j.colsurfb.2021.111881
Received 31 March 2021; Received in revised form 4 May 2021; Accepted 24 May 2021
Available online 28 May 2021

N-dimethylaminoethane)-carbamoyl] cholesterol (DC-Chol) and the zwitterionic helper lipid dioleoylphosphatidylethanolamine (DOPE) and compared its performances to the Lipofectamine gold standard. Irrespective of the vector used for lipofection, cell division was found to be a necessary step to obtain a detectable amount of GFP expressed intracellularly, i.e. DNA nuclear localization shall occur predominantly in cells that are actively replicating, probably favored by the nuclear envelope (NE) breakdown during mitotic prophase [9]. Accordingly, a model was proposed in which the degree of symmetry of protein expression between daughter cells can be linked to the number of DNA copies bioavailable within the cell just before the nuclear breakdown event [9]. Quite unexpectedly, data indicate that a relatively low amount of DNA copies are able to eventually reach the nucleus even after a massive event such as the NE breakdown. In light of this, it is not surprising that, if alternative routes for nuclear entry are exploited by lipofected exogenous DNA, these are also difficult to be deciphered by direct measurements. In other words, these routes might involve such a limited amount of DNA copies that consequent protein expression might fall below the detection limit. Also, in our previous study, only a very limited number of cells per experiment could be monitored over time: as result, the possibility that routes not exploiting the NE breakdown effectively contribute to DNA entry into the nucleus cannot be ruled out. We are tempted to speculate that, if these latter mechanisms are contributing, they might involve DNA direct crossing of the NE barrier by either nuclear pore complex (NPC) translocation or NE local reorganization (e.g. by membrane fusion processes) capable of allowing DNA to bypass the barrier. To tackle these possibilities, here we use a fluorescently-labelled DNA plasmid (Cy3-DNA) to specifically monitor DNA position within the cell at specific time points during the lipofection process. In addition, we use confocal fluorescence microscopy in multi-channel mode to simultaneously detect the exact position of the whole nuclear compartment, labelled with Hoechst, and of the NE barrier in particular. This latter is specifically imaged by exploiting the spectral shift of the fluorescent dye FM4-64 (N-(3-triethylammoniumpropyl)-4-(p-diethylaminophenylhexatrienyl)-pyridinium 2Br). The FM4-64 dye, in fact, belongs to a class of amphiphilic styryl dyes (chemical structure reported, among others, in Ref. [15]) which insert into the outer leaflet of the plasma membrane at physiological temperature and are thought to enter by at least two possible mechanisms: internalization by endocytosis or/and internalization involving flippase and lipid transfer protein activity. Irrespective of the internalization pathway, however, FM4-64 is thought to insert into the lipid bilayer with the polar head close to the hydrophilic lipid phosphate heads, and the mostly hydrophobic core/tail close to the lipid hydrocarbon tails. FM4-64 works as an environment-sensitive dye which it exhibits a detectable fluorescence enhancement upon association to the membrane. Interestingly, it shows enhanced fluorescence at the NE when excited in the 620−650-nm range (at 633 nm in our experiments) with respect to the other membranes of the endo-lysosomal pathway and of the endoplasmic reticulum (ER). These latter, by contrast, are clearly discernible if FM4-64 is excited in the 480−520-nm range [16]. Previous in-vitro data indicated that the dye spectral shift is revelatory of an enrichment of negatively charged lipids at the NE, presumably due to local phospholipid synthesis [17]. As test lipidic formulation, in continuity with previous studies, we choose the patented formulation made of DC-Chol/DOPE mixture, with plasmidic DNA pre-condensed by means of protamine [18]. In fact, based on former extensive characterization, we know that these lipid-protamine-DNA (LPD) nanoparticles (NPs) are stable in solution (please refer to Table 1 for the characterization of size and zeta-potential of all the lipid nanoparticles used in this study) and are efficiently taken up through a combination of both fluid-phase micropinocytosis and clathrin-dependent pathways, then actively transported towards the cell nucleus along microtubules [19]. Of note, during their journey within the cell, these LPD NPs have demonstrated increased ability to escape from the endo-lysosomal pathway as compared to either standard lipoplexes (e.g. DOTAP-DOPC-based ones without protamine) or even analogous LPD NPs but formulated with DOTAP-DOPC (used here as control together with Lipofectamine), which are both extensively trapped into the lysosome compartment for degradation [19]. The peculiar property of DC-Chol/DOPE-based LPD NPs was linked to the membrane-fusogenic activity of the nanocarrier lipidic surface, with a specific role for cholesterol [19,20]. Still, as already mentioned, direct evidence of the real effectiveness of the last step, i.e. nuclear entry of plasmidic DNA, was not reported.

Table 1
Size and zeta-potential of protamine-DNA (PD) microspheres and lipid-protamine-DNA (LPD) nanoparticles.

	Size (nm)	Zeta-potential (mV)
PD	180 ± 17	−19.5 ± 0,7
DC-Chol-DOPE/PD	225 ± 23	31.3 ± 0,3
DOTAP-DOPC/PD	199 ± 14	34.6 ± 2.8
Lipofectamine/PD	217 ± 12	39.7 ± 3.5

2. Results

Here we imaged CHO-K1 cells at 3−6 h post treatment for all the tested formulations, that is: in a time-window just following the one previously found as needed for the endocytic uptake of the chosen formulation (i.e. 0−3h) [20]. By purpose, we excluded from our analysis those cells eventually going through the process of mitotic division during the experiment. Worthy of mention, we did not observe any clear sign of cell death/apoptosis during imaging at the single-cell level for all tested formulations, in keeping with the low overall cytotoxicity measured at the population level at 24 h post-treatment (Suppl. Fig. 1) and in good agreement with previous reports by some of us [19,20]. To start, we performed a 2-channel experiment on cells treated with DC-Chol/DOPE LPD nanoparticles, carried out using Cy3-labelled DNA and Hoechst as a marker of the nucleus. More in detail, we performed optical sectioning of the *xy*-plane of cells with axial resolution of approximately 1 μm. Careful inspection of recorded confocal images reveals Cy3-DNA-positive clusters apparently localized in the nuclear compartment in the vast majority of cells (~95 %). Please note that Cy3-DNA clusters may appear at any *z*-level of the nuclear compartment, depending on the specific cell analyzed (according to cell morphology, nucleus thickness, distance from the petri-dish glass, etc.): it is thus important to scan the entire *z*-axis to probe the presence of clusters. A convenient procedure is by performing a *z*-stack imaging of the cell and then analyze the maximum intensity project (MIP) of the derived images (see Materials and Methods for further details). For instance, in the example in Fig. 1a, apparently only one cell among five shows a Cy3-DNA cluster within the nucleus. However, MIP analysis (see Supp. Fig. 2) reveals that at least three additional cells clearly show Cy3-DNA positive clusters within the nucleus, evidently localized at different z-levels as compared to the one highlighted by the yellow box in Fig. 1a. In general, according to our experimental procedure, once a Cy3-DNA cluster is identified in the nucleus in the *xy*-plane, at any possible z-level, the same cluster is then additionally inspected in the other two orthogonal views (i.e. *yz*-and *xz*-planes) to certify effective nuclear localization. Two outcomes are reported at this stage: *i*) in the vast majority of cases (~90 % of the total of cells with a positive cluster in the *xy*-plane) the analysis of the three orthogonal projections confirms effective nuclear localization of the Cy3-positive cluster (Fig. 1a-b and additional example in Supp. Fig. 3, a–b); *ii*) in the remaining minor fraction of cases the full analysis in the three orthogonal projections reveals mis-localization of the Cy3-DNA clusters in nuclear compartment (see example in Supp. Fig. 3, c–d): in these peculiar cases, in fact, while the *xy*-plane analysis may suggest effective localization of the Cy3-positive cluster in the nucleus, *yz*- and *xz*-projection analyses reveal that the same cluster is localized in a region where the Hoechst signal

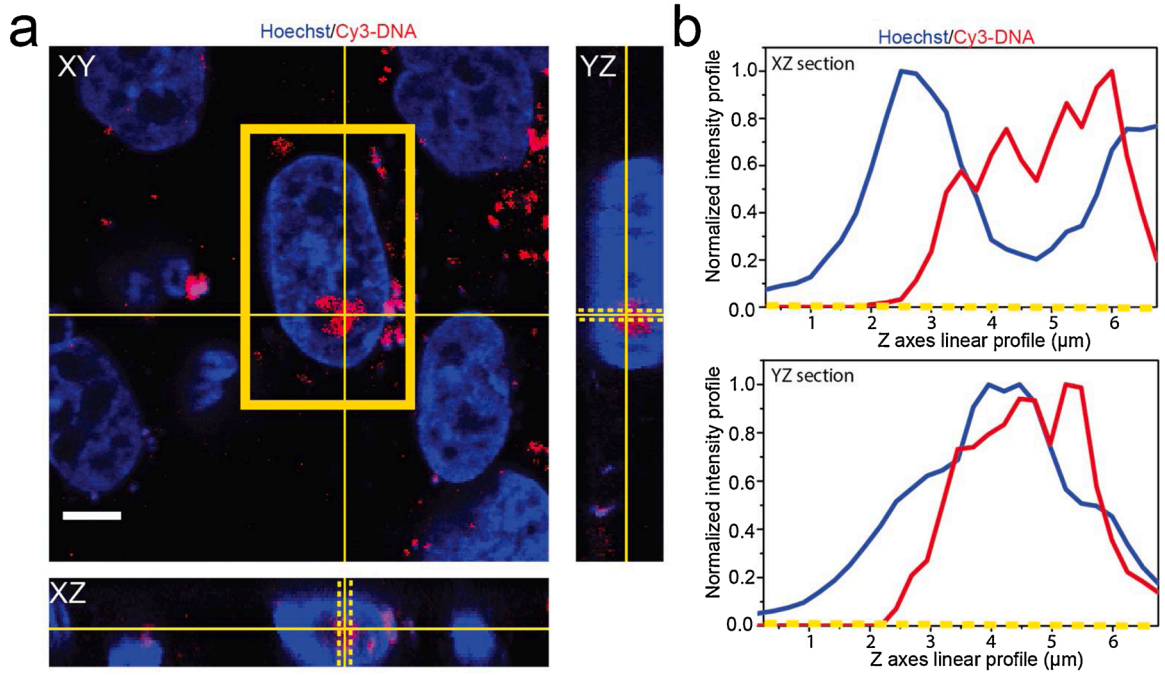

Fig. 1. a) Exemplary XY plane of confocal z-stack acquisition of CHO cells incubated with Cy3-DNA (red signal) and treated with Hoechst Dye 33258 for nuclear staining (blue signal). Orthogonal views (XZ and YZ planes) extracted from z-stack are reported. Scale bar: 5 μ m. **b)** Normalized intensity profile of Cy3 and Hoechst fluorescence signal (red and blue curves, respectively) for XZ and YZ planes. Yellow dotted lines in (A) define the positions along which intensity profiles were plotted.

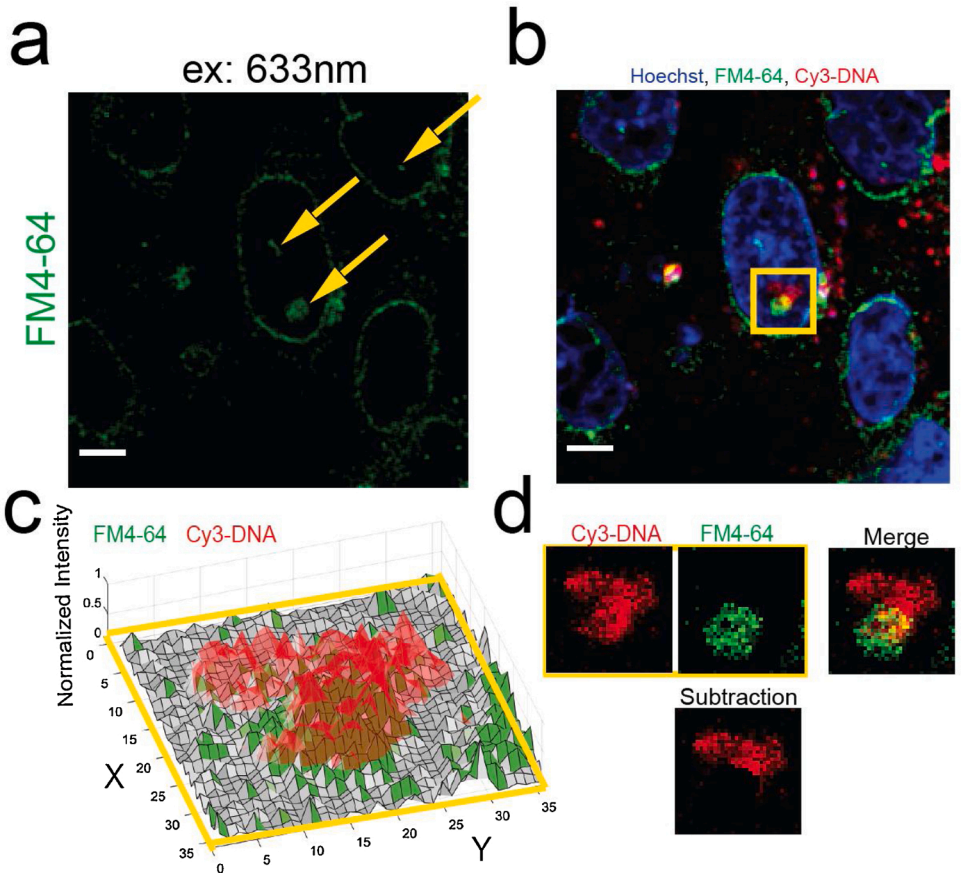

Fig. 2. a) Exemplary image of FM4-64 intracellular staining, excited with a 633 nm laser source (emission collected in the 650-750 nm range), showing the peculiar staining of NE. Yellow arrows identify nuclear invaginations as NE intranuclear extensions. Scale bar: 5 μ m**. b)** Superimposition of Hoechst (blue), FM4-64 (green) and Cy3-DNA (red) signals, showing the colocalization of FM4-64 labelled NE and transfected Cy3-DNA inside the cell nucleus. **c)** Visual inspection of normalized fluorescence signal of FM4-64 and Cy3-DNA in the region defined by 36 × 36 pixels ROI (in yellow in (c)), showing the partial overlapping of the two fluorescence signals. **d)** Zoomed region defines by yellow ROI in (b) showing the superimposition (merge) of the two fluorescence signals and the supposed escaping of Cy3-DNA by FM4-64 labelled NE invaginations, as shown by subtraction of green signal from the red one.

collapse down or is even null, thus likely corresponding to the periphery of the nucleus or even to the cytoplasmic perinuclear region.

As control, we performed similar measurements on cells treated with DOTAP-DOPC-based LPD NPs on one side, and Lipofectamine-based ones on the other. Based on previous data, in fact, the former is a formulation with sensibly lower TE as compared to DC-Chol/DOPE [21], while the latter is a recognized gold standard with very high TE. Interestingly, at 3−6 h post-treatment, our 2-channel experiment with Cy3-labelled DNA and Hoechst reveal the complete absence of Cy3-DNA-positive clusters in the nuclear compartment of cells treated with DOTAP-DOPC LPD NPs: as reported in the exemplary case of Suppl. Fig. 4, we performed confocal scan of the entire *z*-axis of the cell as Cy3-DNA clusters may appear at any *z*-level of the nuclear compartment. By contrast, the same experiment revealed the presence of Cy3-DNA-positive clusters in the nuclear compartment of cells treated with Lipofectamine-based LPD NPs, in analogy with data reported in Fig. 1 for DC-Chol/DOPE (Suppl. Fig. 5).

At this point it is worth noting that, in our opinion, optical imaging of cluster position along the three axes does not provide a definitive proof of cluster effective nuclear localization. In fact, the nuclear clusters observed in the experiment with DC-Chol/DOPE LPD NPs (and Lipofectamine LPD NPs) might be trapped in membranous invaginations of the NE eventually spanning the nuclear compartment. These latter, identified in 1997 by Fricker and collaborators [22], are cell-type specific channels with a morphology/length that varies from single short tubes to multiple, complex, branched structures with a characteristic width in the 100−1000 nm [22,23] and very commonly found in cancer cells [24]. Of note, they were found in 90 % of interphase CHO-K1 cells, in a number of 1–2 per cell nucleus [22], similarly to what observed here. As described above, this intriguing possibility was addressed by adding a channel to our confocal imaging experiments, for the specific imaging of the FM4-64-labelled NE barrier.

In more detail, in these experiments cells are transfected with Cy3-DNA LPD NPs and co-stained with Hoechst and FM4-64, excited at 633 nm to specifically monitor the NE position (Fig. 2a-b, same cell as in Fig. 1). Of note, this experiment reveals that cells with Cy3-DNA clusters with apparent nuclear localization in the three-axes analysis are spatially associated with FM4-64-positive structures, i.e. to NE-specific invaginations spanning across the nucleus. Of note, this happens for all Cy3-postive clusters (we report an additional representative case in Supp. Fig. 6, with the corresponding MIP analysis in Supp. Fig. 7).

Please also note that we obtained similar results on HeLa cells both in terms of positive clusters within the nucleus and their spatial contiguity with the FM4-64-labelled NE (examples in Supp. Fig. 8). Based on these evidences, we are prompted to speculate that all cell types with tubular invaginations of the NE could yield a similar results if treated with fusogenic lipid NP. In general, the observed spatial contiguity between DNA and NE structures shall suggest caution in the interpretation of DNA-localization data based solely on imaging the DNA and the nuclear compartment (e.g. by using standard chromatin labelling). This could in principle generate mis-interpretation of the effective DNA localization, leading in turn to speculate erroneously about DNA transfection capabilities. However, a more detailed analysis of the spatial pattern of the intra-nuclear Cy3-positive and FM4-64-positive clusters reveals that the two signals are not fully superimposed (Fig. 2c-d, see also Supp. Fig. 4). In particular, the Cy3-positive cluster generally occupies a larger area as compared to the FM4-64-positive one, resulting in only partial co-localization of the two signals. This in turn suggests that the DNA delivered by the chosen formulation is not completely trapped within the NE invaginations (and consequently excluded from the nucleus) but instead it could have used those tubular regions as entry-points to the nuclear environment. The low degree of co-localization (see, for instance, the 'subtraction' image in Fig. 2d), together with the observation that NE structures associated with DNA clusters are typically bigger than expected, prompt us to speculate that the mechanism of Cy3-DNA cluster formation could arise from extensive membrane reorganization, a process favored by the high local concentration of lipids (belonging both from the DNA vector, in the form of DC-Chol/DOPE, and from the NE) that could be present at the level of these tubular regions and by the gain in lipid mixing entropy [25–27]. Of particular note, as mentioned above, a similar mechanism was observed for DC-Chol/DOPE DNA formulations (even if in absence of DNA pre-condensation by Protamine) at the level of lysosomes, where large clusters of Cy3-DNA showed only minor co-localization with the lysosomal compartment, a result interpreted again as due to the high fusogenic activity of the DC-Chol/DOPE formulation and linked to its TE [20]. This hypothesis would also help explaining the differential behavior observed here, in terms of the presence of Cy3-DNA intra-nuclear clusters, for less fusogenic formulations, such as DOTAP/DOPC, or similarly high fusogenic ones, such as Lipofectamine.

3. Conclusions

We already know that massive NE breakdown during mitotic division is a major nuclear entry route for exogenous DNA. However, the possibility that routes not exploiting the NE breakdown effectively contribute to DNA entry into the nucleus is supported, among others, by data obtained in non-dividing cells. Thus, it appears clear that getting experimental proof on the existence and nature of these alternative routes is highly desired in the field. Potentially, the identification of the molecular details of these processes could open new perspective for their exploitation by gene-delivery vectors and for the consequent optimization of their TE, particularly for difficult-to-transfect and non-dividing cells. Here we address the process of lipofection by using the DC-Chol/DOPE lipid formulation, with DOTAP/DOPC and Lipofectamine as controls (with DNA pre-condensed by Protamine in all cases) and monitoring directly the localization of fluorescently-labelled DNA plasmids in living interphase (non-dividing) cells. Of note, the vast majority of cells treated with the DC-Chol/DOPE lipid formulation (and, similarly, the vast majority of those treated with Lipofectamine-based LPD NPs) showed clear nuclear localization of Cy3-DNA clusters as result of z-stack reconstruction of the nuclear volume by confocal imaging. By contrast, a similar analysis was not able to reveal any Cy3-positive cluster in the nucleus of cells treated with the DOTAP/DOPC lipid formulation. At this point, by exploiting the spectral shift of the fluorescent dye FM4-64 we selectively identify the position of the nuclear envelope barrier, while concomitantly imaging the whole nuclear compartment (by Hoechst) in a multi-channel 3D confocal imaging experiment. The information added by the FM4-64 channel in cells treated with the DC-Chol/DOPE lipid formulation reveals that the observed DNA clusters are typically associated with the NE membrane in the form of tubular invaginations spanning the nuclear environment. The observation that such Cy3-positive clusters occupy a larger area as compared to the associated NE structures suggests that the DNA may not be completely trapped within the NE tubular invaginations but instead could exploit the same regions as entry-points towards the nuclear environment, maybe following the same extensive membrane reorganization/fusion processes already observed at the level of the endo-lysosomal pathway [20]. These considerations would in turn offer the rationale to explain why cells treated with DOTAP/DOPC-based LPD NPs did not show nuclear clusters: such formulation, in fact, is much less fusogenic as compared to DC-Chol/DOPE and would then be more favorably destined to trapping and degradation in the endo-lysosomal compartments rather than reach the NE tubular structures. Not surprisingly, by contrast, the highly fusogenic Lipofectamine formulation closely resembles DC-Chol/DOPE in terms of the presence of clusters in the nucleus. Future experiments will be tailored to understand if what observed here constitutes an effective nuclear-entry route available for exogenous lipofected plasmidic DNA that is independent from nuclear breakdown and how much it contributes to the final TE.

4. Materials and methods

4.1. Cell culture, labelling procedure and viability tests

CHO-K1 cells (purchased from American Type Culture Collection CCL-61 ATCC) were grown in DMEM Ham's F12 K medium, supplemented with 10 % of fetal bovine serum and 100 U/mL penicillin, 100 mg/mL streptomycin (Invitrogen) at 37 °C and 5% CO_2. CHO cell line was chosen due to its common use in research, especially for expression, transfection, and recombinant protein production.

To stain the nuclear compartment, cells were treated with Hoechst 33342 (2 μg/mL) for 10 min before confocal microscopy experiments. FM4-64 (Life Technologies) was used to stain endocytic compartments, Endoplasmatic Reticulum and Nuclear Envelope. It was dissolved in DMSO and added to plated cells at a final concentration of 20 μM in complete DMEM F12 for 30 min at 37 °C. Cells were then washed once with PBS and further incubated in complete medium.

For cell viability tests, 10^4 cells were seeded in 96-well plates and allowed to adhere for 12 h. Cell cultures were exposed to P/DNA microspheres and LPDs for 48-h, followed by MTT [3-(4,5-dimethylthiazol-2-yl)-2,5-diphenyltetrazolium bromide] (Sigma Aldrich, AL, USA). Briefly, 5 mg/mL MTT in 100 μL of DMEM without phenol red was added to the cultured cells for 2-h. Cells were washed by phosphate buffered saline (PBS) and lysed by 100 mL of dimethyl sulfoxide (DMSO). The concentration of MTT was examined colorimetrically; absorbance was determined at 570 nm. Results are given as average ± standard deviation of three independent replicates.

4.2. Cationic liposomes

Cationic lipids 1,2-dioleoyl-3-trimethylammonium-propane (DOTAP) and (3β- [N-(N′,N′-dimethylaminoethane)-carbamoyl])-cholesterol (DC-Chol) and neutral helper lipids 1,2-dioleoyl-sn-glycero-3-phosphocholine (DOPC) and (DOPE) were purchased from Avanti Polar Lipids (Alabaster, AL, USA) and used without further purification. Cationic liposomes (CLs) were prepared by the thin lipid film method. In brief, the proper amount of lipids was dissolved in chloroform, and the solvent was evaporated under vacuum for 24 h. The obtained lipid film was hydrated with the appropriate amount of Tris-HCl buffer solution (10 − 2 M, pH 7.4) to achieve the desired final concentration (1 mg/mL). Liposome dispersion was sonicated to clarity to prepare small unilamellar vesicles (SUVs).

4.3. Lipid-protamine-DNA nanoparticles

Protamine sulfate salt (P) from salmon (MW =5.1 kDa) was purchased from Sigma-Aldrich (St. Louis, MO, USA). P/DNA microspheres were prepared by incubating positively charged P with negatively charged DNA for 20 min at room temperature (P/DNA weight ratio, $R_W = 0.5$). To prepare LPD NPs, P/DNA microspheres were incubated with i) DC-Chol-DOPE CLs, ii) DOTAP-DOPC CLs and iii) Lipofectamine®. LPD NPs from DOTAP-DOPC and DC-Chol-DOPE CLs were prepared at cationic lipid/DNA charge ratio $\rho = 4$, while proper amount of Lipofectamine® was set according to manufacturer's indications. After pipetting up and down a few times, LPD NPs were extruded 20 times through a 0.2 μm polycarbonate carbonate filter by using the Avanti Mini-Extruder (Avanti Polar Lipids, Alabaster, AL). After preparation, LPD NPs were kept at room temperature for 15−30 min before use.

4.4. Lipoplexes preparation and trasfection

Size and zeta-potential of P/DNA microspheres and LPD NPs were measured at 25 °C by a Malvern ZetaSizer Nano spectrometer equipped with a 5 mW He − Ne laser (wavelength λ =632.8 nm) and a digital logarithmic correlator, which allows to estimate the hydrodynamic radius of particles (Table S1). The same apparatus was used to measure zeta-potential. For each sample, three independent measurements were averaged. Results are given as average ± S.D.

4.5. Lipoplexes trasfection procedure

For transfection of Protamine-based lipo-complexes, cells were plated onto a 35-mm glass-bottom dish (WillCo-dish GWSt-3522) to be 70–90 % confluent 24 h prior to transfection. First salmon extracted protamine sulfate salt (Sigma-Aldrich St. Louis, MO, USA) was dissolved (MW =5.1 kDa) in distilled water to a final concentration of 0.5 mg/mL and incubate for 24 h at 4 °C. The day of transfection, plasmid DNA and protamine were mixed and incubate for 30 min at RT, then Dc-Chol/DOPE lipids (or DOTAP/DOPC, or Lipofectime) were added to protamine/DNA complexes and incubate for 30 min at RT. Finally lipid/protamine/DNA complexes were added to cells in serum-free medium and incubated for 3 h at 37 °C.

4.6. Fluorescence confocal imaging and colocalization analysis

Confocal fluorescence microscopy experiments were performed with the Olympus Fluoview 1000 (Olympus, Melville, NY) confocal microscope. After 3 h from transfection, glass bottom dishes (WillCo-dish GWSt-3522) containing transfected cells were mounted in a temperature-controlled chamber at 37 °C and 5% CO_2. Imaging of Hoechst 33342, Cy3-DNA LPD NPs and FM4-64 was performed exciting, respectively, with 405, 543 and 633 nm and acquiring fluorescence signals between 410–480, 550–600 and 650−750 nm. To avoid the presence of any cross-talk and/or bleed-through among channels, the signals were acquired in 'sequential mode', i.e. with just one laser and detection channel alternatively turned on. To perform Z-stack acquisitions, typically 30 optical planes were acquired for each field of view, with a step of 0.25 μm/slice. Z-stacks were used to reconstruct the fluorescence intensity distributions along XZ and YZ planes, orthogonally with respect XY plane, as shown in figures and along chosen linear profile, to determine whether liposomal particles are localized inside (or not) the nuclear compartment. Image analysis was carried out by means of ImageJ software. Briefly, fluorescence counts were plotted as z-values in a three-dimensional matrix for both channels. Image subtraction was carried out subtracting green channel intensity values from the red channel using ImageJ plugin Image Calculator. Maximum intensity projection (MIP) analysis was used to probe the presence of Cy3-DNA clusters at any z-level within the nucleus. MIP is a method for z-stack experiments that consists in projecting the three dimensional pixel (i.e. voxel) with the highest intensity value for each z-plane/level onto a single 2D image. MIP was performed using the ImageJ appropriate tool.

CRediT authorship contribution statement

Gianmarco Ferri and **Giuseppe Fiume:** performed research, analyzed data, wrote the manuscript; **Daniela Pozzi:** analyzed data, revised the manuscript; **Giulio Caracciolo:** designed research, analyzed data, wrote the manuscript; **Francesco Cardarelli:** designed research, supervised research, analyzed data, wrote the manuscript.

Funding

This research was partly funded by MIUR PRIN Grant (*2017YF9FBS*) to F.C.

Declaration of Competing Interest

The authors declare that they have no known competing financial interests or personal relationships that could have appeared to influence the work reported in this paper.

Appendix A. Supplementary data

Supplementary material related to this article can be found, in the online version, at doi:https://doi.org/10.1016/j.colsurfb.2021.111881.

References

[1] H. Bai, G.M.S. Lester, L.C. Petishnok, D.A. Dean, Cytoplasmic transport and nuclear import of plasmid DNA, Biosci. Rep. 37 (6) (2017), https://doi.org/10.1042/BSR20160616 pag. BSR20160616, dic.

[2] M.R. Capecchi, High efficiency transformation by direct microinjection of DNA into cultured mammalian cells, Cell 22 (2) (1980) 479–488, https://doi.org/10.1016/0092-8674(80)90358-x. Pt 2 nov., pagg.

[3] M. Graessmann, J. Menne, M. Liebler, I. Graeber, A. Graessmann, Helper activity for gene expression, a novel function of the SV40 enhancer, Nucleic Acids Res. 17 (16) (1989) 6603–6612, https://doi.org/10.1093/nar/17.16.6603, ago.

[4] J. Zabner, A.J. Fasbender, T. Moninger, K.A. Poellinger, M.J. Welsh, Cellular and molecular barriers to gene transfer by a cationic lipid, J. Biol. Chem. 270 (32) (1995) 18997–19007, https://doi.org/10.1074/jbc.270.32.18997, ago.

[5] R. Mirzayans, R.A. Aubin, M.C. Paterson, Differential expression and stability of foreign genes introduced into human fibroblasts by nuclear versus cytoplasmic microinjection, Mutat. Res. 281 (2) (1992) 115–122, https://doi.org/10.1016/0165-7992(92)90045-j, feb.

[6] A.M. Thorburn, A.S. Alberts, Efficient expression of miniprep plasmid DNA after needle micro-injection into somatic cells, BioTechniques 14 (3) (1993) 356–358, mar.

[7] D.A. Dean, B.S. Dean, S. Muller, L.C. Smith, Sequence requirements for plasmid nuclear import, Exp. Cell Res. 253 (2) (1999) 713–722, https://doi.org/10.1006/excr.1999.4716, dic.

[8] J.J. Ludtke, M.G. Sebestyén, J.A. Wolff, The effect of cell division on the cellular dynamics of microinjected DNA and dextran, Mol. Ther. J. Am. Soc. Gene Ther. 5 (5) (2002) 579–588, https://doi.org/10.1006/mthe.2002.0581. Pt 1 mag.

[9] G. Fiume, C. Di Rienzo, L. Marchetti, D. Pozzi, G. Caracciolo, F. Cardarelli, Single-cell real-time imaging of transgene expression upon lipofection, Biochem. Biophys. Res. Commun. 474 (1) (2016) 8–14, https://doi.org/10.1016/j.bbrc.2016.03.088, mag.

[10] L.D. Cervia, C.-C. Chang, L. Wang, M. Mao, F. Yuan, Enhancing electrotransfection efficiency through improvement in nuclear entry of plasmid DNA, Mol. Ther. - Nucleic Acids 11 (2018) 263–271, https://doi.org/10.1016/j.omtn.2018.02.009, giu.

[11] S. Brunner, T. Sauer, S. Carotta, M. Cotten, M. Saltik, E. Wagner, Cell cycle dependence of gene transfer by lipoplex, polyplex and recombinant adenovirus, Gene Ther. 7 (5) (2000) 401–407, https://doi.org/10.1038/sj.gt.3301102, mar.

[12] B.D. Hornstein, D. Roman, L.M. Arévalo-Soliz, M.A. Engevik, L. Zechiedrich, Effects of circular DNA length on transfection efficiency by electroporation into HeLa cells, PLoS One 11 (12) (2016) e0167537, https://doi.org/10.1371/journal.pone.0167537, dic.

[13] A. Fasbender, J. Zabner, B. Zeiher, M. Welsh, A low rate of cell proliferation and reduced DNA uptake limit cationic lipid-mediated gene transfer to primary cultures of ciliated human airway epithelia, Gene Ther. 4 (11) (1997) 1173–1180, https://doi.org/10.1038/sj.gt.3300524, nov.

[14] G. Grandinetti, T.M. Reineke, Exploring the mechanism of plasmid DNA nuclear internalization with polymer-based vehicles, Mol. Pharm. 9 (8) (2012) 2256–2267, https://doi.org/10.1021/mp300142d, ago.

[15] S. Fischer-Parton, R.M. Parton, P.C. Hickey, J. Dijksterhuis, H.A. Atkinson, N. D. Read, Confocal microscopy of FM4-64 as a tool for analysing endocytosis and vesicle trafficking in living fungal hyphae, J. Microsc. 198 (3) (2000) 246–259, https://doi.org/10.1046/j.1365-2818.2000.00708.x, giu.

[16] P.a.C. van Gisbergen, A. Esseling-Ozdoba, J.W. Vos, Microinjecting FM4-64 validates it as a marker of the endocytic pathway in plants, J. Microsc. 231 (2) (2008) 284–290, https://doi.org/10.1111/j.1365-2818.2008.02041.x, ago.

[17] T. Zal, M.A. Zal, C. Lotz, C.J. Goergen, N.R.J. Gascoigne, Spectral shift of fluorescent dye FM4-64 reveals distinct microenvironment of nuclear envelope in living cells, Traffic Cph. Den. 7 (12) (2006) 1607–1613, https://doi.org/10.1111/j.1600-0854.2006.00498.x, dic.

[18] G. Caracciolo, D. Pozzi, C. Marchini, A. Amici, Multicomponent Lipid Nanoparticles and Processes for the Preparation Thereof, WO/2014/057432, 2021.

[19] D. Pozzi, et al., Mechanistic understanding of gene delivery mediated by highly efficient multicomponent envelope-type nanoparticle systems, Mol. Pharm. 10 (12) (2013) 4654–4665, https://doi.org/10.1021/mp400470p, dic.

[20] D. Pozzi, et al., Transfection efficiency boost of cholesterol-containing lipoplexes, Biochim. Biophys. Acta 1818 (9) (2012) 2335–2343, https://doi.org/10.1016/j.bbamem.2012.05.017, set.

[21] D. Pozzi, et al., Mechanistic evaluation of the transfection barriers involved in lipid-mediated gene delivery: Interplay between nanostructure and composition, Biochim. Biophys. Acta BBA - Biomembr. 1838 (3) (2014) 957–967, https://doi.org/10.1016/j.bbamem.2013.11.014, mar.

[22] M. Fricker, M. Hollinshead, N. White, D. Vaux, Interphase nuclei of many mammalian cell types contain deep, dynamic, tubular membrane-bound invaginations of the nuclear envelope, J. Cell Biol. 136 (3) (1997) 531–544, https://doi.org/10.1083/jcb.136.3.531, feb.

[23] I. Schoen, L. Aires, J. Ries, V. Vogel, Nanoscale invaginations of the nuclear envelope: shedding new light on wormholes with elusive function, Nucl. Austin Tex. 8 (5) (2017) 506–514, https://doi.org/10.1080/19491034.2017.1337621, set.

[24] A.N. Malhas, D.J. Vaux, Nuclear envelope invaginations and cancer cancer, in: E. C. Schirmer, J.I. de las Heras (Eds.), Biology and the Nuclear Envelope, vol. 773, Springer New York, A c. di New York, NY, 2014, pp. 523–535.

[25] G. Caracciolo, D. Pozzi, R. Caminiti, e H. Amenitsch, Two-dimensional lipid mixing entropy regulates the formation of multicomponent lipoplexes, J. Phys. Chem. B 110 (42) (2006) 20829–20835, https://doi.org/10.1021/jp0620926, ott.

[26] D. Pozzi, et al., Toward the rational design of lipid gene vectors: shape coupling between Lipoplex and anionic cellular lipids controls the phase evolution of Lipoplexes and the efficiency of DNA release, ACS Appl. Mater. Interfaces 1 (10) (2009) 2237–2249, https://doi.org/10.1021/am900406b, ott.

[27] C. Marchini, et al., Tailoring lipoplex composition to the lipid composition of plasma membrane: a trojan horse for cell entry? Langmuir 26 (17) (2010) 13867–13873, https://doi.org/10.1021/la1023899, set.